

# Photocleavable side groups to spatially alter hydrogel properties and cellular interactions

Vyas V. Ramanan,<sup>†</sup> Joshua S. Katz,<sup>†</sup> Murat Guvendiren, Eric R. Cohen, Ross A. Marklein and Jason A. Burdick\*

Received 17th March 2010, Accepted 8th June 2010

DOI: 10.1039/c0jm00734j

Hydrogel systems with inducible variations in mechanical and chemical properties are of interest to many aspects of tissue engineering. Substrate-tethered hydrogel films, fabricated by copolymerization of hydroxyethylacrylate with the photolabile monomer 2-nitrobenzyl acrylate (2-NBA) and a crosslinker were shown to be responsive to UV light through cleavage of the 2-NBA moiety. The surface and bulk properties of the films were characterized by infrared spectroscopy and atomic force and confocal microscopy. At long irradiation times, a tripling of the swelling ratio and an order of magnitude decrease in gel modulus were observed, coupled with an increase in surface wettability. Following short exposures, the gels became resistant to protein and cell adhesion, a trend that was reversed with longer exposure times. Finally, high-fidelity patterns of gel swelling were fabricated through spatially selective irradiation by employing basic photomasks. These materials are useful for future studies for which spatial and temporal control of material properties and cellular interactions are desirable.

## Introduction

Spatial control of material properties at resolutions down to the micro-scale is of great importance for numerous fields. Micro-patterning with lithographic techniques has long been applied to electronics,<sup>1</sup> photonics,<sup>2</sup> and microfluidics,<sup>3</sup> but only recently have technological advances in this area been translated to biological systems for smart drug delivery and tissue engineering applications.<sup>4–6</sup> Cells are well known to respond to complex combinations of cues such as substrate mechanics, ligand presentation, and soluble molecules.<sup>7</sup> Consequently, the design of substrates that present one or more of these factors in a spatial or temporal manner is of great benefit to the study of cellular behavior and for tissue engineering.

Several tissue engineering approaches have focused on providing cells with a spatially defined microenvironment to influence outcomes such as adhesion, proliferation, and differentiation. Differential cellular responses have been observed using materials with patterned mechanics<sup>8</sup> and adhesion peptide presentation.<sup>9</sup> Additionally, cell outgrowth<sup>10</sup> and infiltration<sup>11</sup> have been directed by the spatial patterning of hydrogels. Higher-order cell functions may also be induced by spatial patterning of cell substrates. For example, T-cell activation was induced or precluded by patterns of multiple proteins in various arrangements.<sup>12</sup> With these approaches in mind, spatially controlling cells may become very important in the engineering of multi-cellular and complex tissues.

Light is an attractive choice for fabricating biomaterial patterns due to the high spatial resolution that is afforded (using masks, digital micro-mirror arrays<sup>13</sup> or laser light<sup>9</sup> for 2-D patterning and two-photon irradiation for 3 dimensions<sup>14</sup>), low

costs and speed of processing, and ease of production on the benchtop.<sup>15</sup> Additionally, the recent development of near-UV responsive moieties has enabled patterning in the presence of cells, while limiting concerns of UV-induced cytotoxicity.<sup>16,17</sup> Using light, changes in chemical structures,<sup>18</sup> mechanics,<sup>8,17</sup> crosslinking,<sup>19,20</sup> solubility,<sup>21</sup> and functional group presentation<sup>22,23</sup> have all been demonstrated for biological systems.

The majority of recent work on spatial patterning and cellular behavior has focused on the tethering of ligands to surfaces, while the effects of substrate mechanics and surface wettability have not been extensively investigated.<sup>24,18,25</sup> In this work, we explored a novel route that uses light to alter substrate chemical and mechanical properties in tandem. We fabricated and characterized hydrogels of poly-(hydroxyethylacrylate-co-2-nitrobenzyl acrylate) before and after exposure to light. Specifically, we investigated properties such as gel swelling, wettability, mechanics, and cell responses with unexposed films, as well as those with short and long-term light exposure. Using hydrogels as the substrate enabled changes in hydrophilicity to induce significant changes in mechanical properties that cannot be accessed through simple patterning of rigid substrates such as glass or silicon. Cell responses indicate a complex interplay between substrate hydrophilicity and mechanics in determining adhesion and proliferation. Finally, the demonstrated ability to spatially and temporally pattern these materials could further improve our ability to mimic various cellular niches *in vitro*.

## Materials and methods

### Synthesis of 2-nitrobenzylacrylate (2-NBA)

2-Nitrobenzyl acrylate (2-NBA) was synthesized in the same manner as has been previously reported for 2-nitrobenzyl methacrylate.<sup>23</sup> Briefly, a 500 mL 3-neck round-bottom flask

Department of Bioengineering, University of Pennsylvania, Philadelphia, PA, 19104, USA. E-mail: burdick2@seas.upenn.edu

<sup>†</sup> Contributed equally to this work.

equipped with an addition funnel was charged with 15 g 2-nitrobenzyl alcohol (98 mmol, Sigma), 150 mL dichloromethane dried over molecular sieves, and 15 mL triethylamine (10.89 g, 107 mmol, Sigma). The addition funnel was filled with 8.9 mL acryloyl chloride (10 g, 110 mmol, Sigma) in approximately 50 mL dichloromethane, and the solution was added drop wise while on ice. The reaction was allowed to proceed for 16 hours at 4 °C. Triethylammonium salts were filtered and the dichloromethane was removed *via* rotary evaporation. The crude product was purified by flash chromatography in ethyl acetate : hexane (1 : 6) as the loading and running solvent. Rotary evaporation yielded the final product as a greenish-yellow oil. <sup>1</sup>H NMR spectra were recorded on a Bruker DMX 360 MHz spectrometer. *J*-coupling constants are reported in Hz.  $\delta_{\text{H}}$  (360 MHz, CDCl<sub>3</sub> (7.27)) 5.63 (2 H, s, CH<sub>2</sub>Ph), 5.93 (1H, dd, *J*<sub>1,2</sub> 10.4, *J*<sub>1,3</sub> 1.4, CH<sub>2</sub>=CH-), 6.23 (1H, dd, *J*<sub>2,1</sub> 10.4, *J*<sub>2,3</sub> 17.3, CH-CH<sub>2</sub>), 6.51 (1H, dd, *J*<sub>3,1</sub> 1.4, *J*<sub>3,2</sub> 17.3, CH<sub>2</sub>=CH-), 7.51 (1H, td, *J* 1.4 and 7.6, Ph-H(4)), 7.63 (2H, m, Ph-H(5) and Ph-H(6)), 8.13 (1H, dd, *J* 1.1 and 7.9, Ph-H(3)).

### Methacrylated slide preparation

Glass coverslips were methacrylated to allow for covalent attachment of gels. 22 mm × 22 mm coverslips were sonicated for 10 min in 10 M NaOH and rinsed with deionized water. Next, 3-(trimethoxysilyl)propyl methacrylate (Sigma) was added to the surface of each slide and reacted at 100 °C for 1 h, followed by 110 °C for 10 min. Finally, the slides were rinsed with deionized water and allowed to dry.

### Preparation of polymer films

The prepolymer solution consisted of 79.5% (v/v) 2-hydroxyethylacrylate (Sigma), 20% (v/v) 2-NBA, 0.5% (v/v) ethylene glycol dimethacrylate (Polysciences) and 1 mg mL<sup>-1</sup> 2,2-azobisisobutyronitrile (Sigma). Films were produced by pipetting the prepolymer solution between a methacrylated coverslip and glass slide separated by a spacer (~0.15 mm) and initiating polymerization by incubating the samples at 65 °C for 60 minutes. Irradiation was accomplished using a UV lamp (EXFO) with a collimating adapter and filters for 320–390 nm. During irradiation, the films were immersed in DMSO, which was replaced every 15 minutes to remove any cleaved molecules. Patterned gels were produced with UV exposure through a TEM grid (TedPella, 200 mesh copper) placed on the film surface. Following exposure, the samples were swelled in DMSO overnight to remove the liberated nitrosobenzyl byproducts. Samples were then washed in several exchanges of deionized water before transfer to the desired final solution. Samples for material characterization were transferred to PBS (pH 7.4, ~270 mOsm). After overnight storage in PBS, 5 samples for investigation of pH-responsiveness were transferred into buffers of varying pH (pH 1.8 was HCl, pH 3.9 and 4.9 were acetate buffer, and pH 7.2 and 8.9 were PBS). Samples used for cell culture were sterilized by heating to 140 °C for 2 hours, transferred to 6-well cell culture dishes, and exposed to a germicidal lamp for 1 hour. Finally, the gels were incubated in a 20 µg mL<sup>-1</sup> fibronectin (Sigma) in PBS solution overnight prior to cell seeding.

### Surface characterization

Static water contact angles were determined using the sessile drop method with a contact-angle meter (Contact Angle Meter, Tanteq) at room temperature. A ~10 µL droplet of water was placed on the surface of the film and the contact angle was determined using the half-angle method. 10 measurements were recorded at different points on the film surface for each exposure time, and the resulting mean and standard deviation of the measurements are reported. The films' surface chemical composition was determined by Fourier transform infrared spectroscopy (FTIR, Nicolet 6700, Thermo Electron Corp). A thin film of substrate-adherent polymer was placed on a zinc selenide crystal and spectra were recorded in attenuated total reflectance (ATR) FTIR mode. The ATR-FTIR spectra were then analyzed to monitor variations in the areas of the nitro peaks (~1530 cm<sup>-1</sup>) normalized to the carbonyl peak (~1730 cm<sup>-1</sup>) with increasing UV exposure times. Swelling-induced surface wrinkling patterns were characterized by optical microscopy on a Zeiss Axiovert 200 inverted microscope, and the wrinkles' characteristic wavelength  $\lambda_c$  was measured in ImageJ (1.41n, National Institutes of Health, Bethesda, MD) by taking 10 measurements for each time point.

### Characterization of swelling and mechanics

Gel swelling ratios were determined with confocal microscopy (Nikon TE300 inverted microscope fitted with a Bio-Rad Radiance 2000 MP3 system, Bio-Rad Laboratories, Inc.). Images were observed through a 10× and/or 20× objective, and recorded with Lasershar 2000 software (Bio-Rad Laboratories, Inc.). Gels were equilibrated in a 0.32 µg mL<sup>-1</sup> FITC in PBS solution for several days to obtain contrast (gels appeared green under fluorescent light). Depth profiles were obtained by collecting *xz*-scans with a 1 mm step size and distances were determined in ImageJ. Hydrogel surface mechanics were quantified using atomic force microscopy (AFM, Veeco Bioscope I). A silicon bead AFM tip with a spring constant of 0.06 N m<sup>-1</sup> was used to obtain force curves for individual points on the gels (10 points chosen for each condition) from which a local elastic modulus was calculated.

### Cell culture

NIH 3T3 fibroblasts (ATCC) were maintained in Dulbecco's Modified Eagle Medium (DMEM, Gibco) supplemented with 10% bovine calf serum (ATCC), 1% sodium bicarbonate (Gibco), and 1% pen/strep (Gibco) in a humidified sterile incubator at 37 °C and 5% CO<sub>2</sub>. 4 hours prior to seeding on the gels, cells were stained with CellTracker Green (Invitrogen). Briefly, 20 µg CellTracker Green was dissolved in 50 µL sterile DMSO and diluted into 10 mL cell media, which was then incubated with the cells for 4 hours. The media was aspirated and the cells were rinsed with PBS, trypsinized, and collected *via* centrifugation. Finally, cells were resuspended in fresh media and seeded on the gels at 100 000 cells per well. Images were collected at 24 and 48 hours on an Olympus BX51 fluorescent microscope. Cell counts were performed using ImageJ for five random points on 3 gels per sample set. Data are presented as means and standard error.

## Statistics

Data for mechanics, surface characterization, and swelling were analyzed by one-way ANOVA with Bonferroni-Holm post-hoc analysis using Excel with Daniel's XL Toolbox Add-In (Daniel Kraus, Cambridge, MA). For cell studies, data were analyzed by one-way ANOVA with Tukey's post-hoc analysis using JMP software (SAS Institute, Cary, NC). For all studies,  $p$ -values of less than 0.05 were considered to be statistically significant.

## Results and discussion

The importance of spatially and temporally defined patterns of material properties in physiological systems is becoming apparent in many biological systems.<sup>14,20,26</sup> By externally modulating gel mechanics and surface properties, it can be possible to define specific areas or time intervals of differential cell response, but this is only possible with advances in material development. This study seeks to characterize the evolution of bulk and surface properties of hydrogels that contain photocleavable hydrophobic side-groups, where light exposure alters network hydrophobicity, material properties, and cellular interactions through liberation of the nitrobenzyl group. Since this process occurs with light, spatial control or the extent and timing of light exposure is readily performed to produce a wide variety of material formulations.

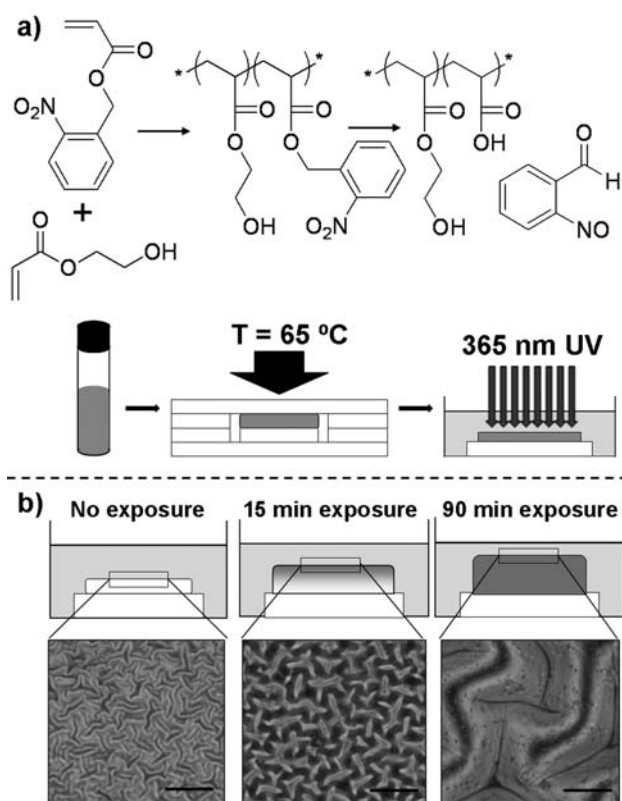


**Fig. 1** Schematic of gel formation and light exposure. (a) Thermal polymerization of HEA and 2-NBA is followed by irradiation with 365 nm UV light in DMSO to cleave 2-nitrobenzyl groups, leaving behind poly (HEA-co-AA). The crosslinking is not shown in the structure. (b) Polymer swelling in PBS is dependent on UV exposure and causes stress-induced wrinkling patterns on the gel surface. The wrinkle morphology is dependent on the time of light exposure. All scale bars = 100  $\mu$ m.

## Surface characterization

A general scheme for preparation of the hydrogel films is presented in Fig. 1. The network is formed from a monoacrylated monomer, a crosslinker, and the pendant photocleavable group. UV irradiation of the network induced cleavage of the 2-nitrobenzyl group, liberating free carboxylic acids and significantly altering the chemical composition of the gel. To explore the kinetics of this reaction, gels were characterized by FTIR spectroscopy as a function of UV exposure time. The asymmetric N–O stretch at 1530  $\text{cm}^{-1}$  was monitored and normalized to the constant carbonyl stretch at 1740  $\text{cm}^{-1}$  (Fig. 2). A steady decrease in the nitro peak is observed with time, with near-complete disappearance of the peak by 90 minutes. As we hypothesized that material properties could be controlled by the degree of nitrobenzyl cleavage, these data suggest that the chemical composition on the surface can be controlled as a function of irradiation time. To further explore this hypothesis, we chose three times for irradiation in future studies—0, 15 and 90 minutes to represent a spectrum of material compositions.

## Wettability, swelling, and mechanics

UV exposure of the gels induces cleavage of the hydrophobic nitrobenzyl groups from the network, liberating hydrophilic acrylic acid side chains that are then free to present themselves on

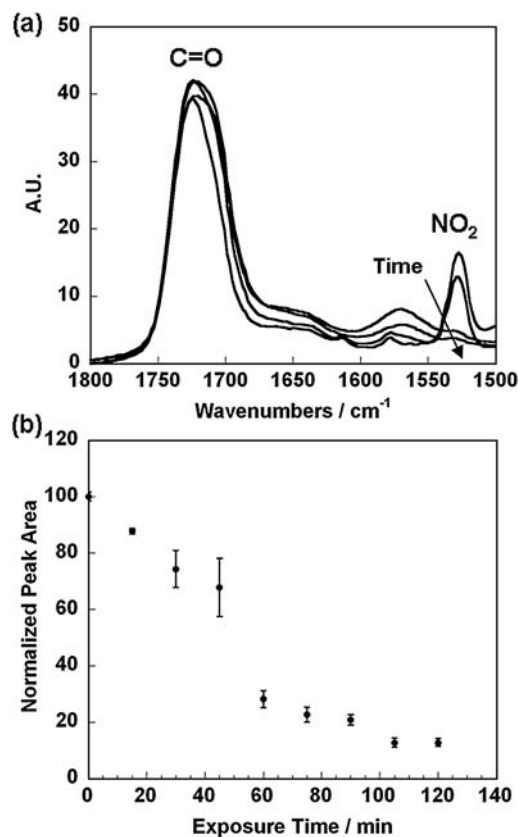


**Fig. 2** (a) FTIR plots of gels after UV exposure times of 0, 45, 90, and 105 min. Note the decrease in peak at 1530  $\text{cm}^{-1}$  due to 2-nitrobenzyl cleavage with time of light exposure. (b) Normalized area of the  $\text{NO}_2$  stretch peak as a function of UV exposure time.

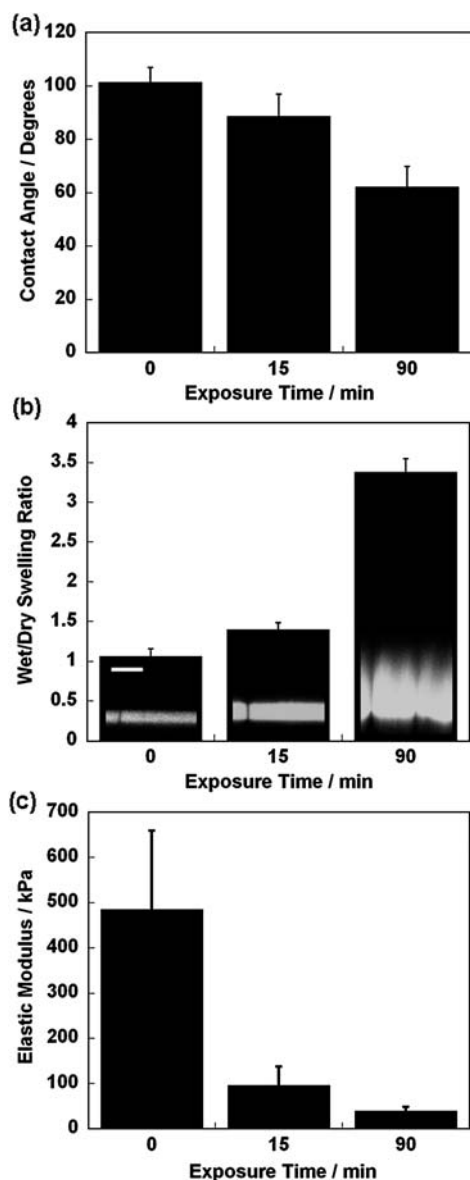


**Fig. 3** (a) Water contact angle on surface of polymer films, (b) Wet/dry swelling ratio measured with film thickness, and (c) elastic modulus in PBS of polymer films after 0, 15, and 90 minutes of UV exposure. The images in (b) are confocal images of the  $xz$ -plane superimposed on the numerical data. Scale bar = 200  $\mu\text{m}$ .  $p < 0.005$  between all groups in (a) and (c) and  $p < 0.05$  between all groups in (b).

the surface to minimize interfacial tension with surrounding water. To investigate the change in surface hydrophilicity following UV exposure, the static water contact angle (WCA) of the surface of dehydrated gels was measured (Fig. 3a). We observed a significant drop in the WCA as gels were exposed to increasing amounts of UV light, with unexposed gels having a moderately hydrophobic WCA of  $101.5^\circ$ , decreasing to  $88.6^\circ$  after 15 minutes of light exposure, and decreasing again to  $62.1^\circ$  after 90 minutes total exposure. The similarity of this final WCA to previously reported WCA values for poly(acrylic acid) (just under  $60^\circ$ ) further corroborates the FTIR data above that show complete or near-complete removal of nitrobenzyl groups from the gel surface.<sup>27</sup> Additionally, the change in WCA of nearly  $40^\circ$

represents a large change in wettability that could potentially be exploited for use with biological systems.

As the gels are covalently attached to the glass substrate, they are constrained to swelling only in the perpendicular direction. Therefore, the volumetric swelling is equal to the linear swelling ( $W$ ) in constrained gels, which can be measured from the ratio of the height of the equilibrated hydrogel ( $h_w$ ) to that of the dry gel ( $h_0$ ) ( $W = h_w/h_0$ ). To measure the swelling ratio, the height of the gels was measured by confocal microscopy before and after swelling in PBS containing FITC ( $0.32 \mu\text{g mL}^{-1}$ ). The swelling ratio increased significantly with exposure time ( $t$ ), from  $W = 1.06$  at  $t = 0$ , to  $W = 1.40$  at  $t = 15$  minutes, to  $W = 3.38$  at  $t = 90$  minutes (Fig. 3b).

We next investigated if the sharp increase in gel swelling was complemented by a matching change in mechanical properties (Fig. 3c). Prior to UV exposure the elastic modulus was 485 kPa, but this decreased to 95.5 kPa after 15 minutes irradiation and 39.4 kPa after 90 minutes. There is clearly a correlation between increased exposure times and increased hydrophilicity—both on the surface and in the bulk—that translates to a sharp decrease in the elastic modulus due to enhanced swelling and decreased crosslinking density. However, the increased swelling may be due to both the decreased hydrophobicity with removal of the nitrobenzyl moiety and the introduction of charged species to the gel. To address this issue, we again performed AFM measurements on films before and after 90 minutes UV exposure, but this time with the gels swollen in buffers at a range of pH values (Fig. 4). At sufficiently low pH values below the  $\text{p}K_a$  of acrylic acid ( $\text{p}K_a \approx 4.2$ ), the liberated acid groups would become protonated, removing any charge in the system. Consequently, changes in the moduli at lower pH would be primarily explained by the hydrophilic character due to the removal of the nitrobenzyl groups without the introduction of charge. However, at low pH, the modulus of the exposed gels matched the moduli of unexposed gels. Only at the pH transition from 4 to 5 (around the  $\text{p}K_a$  of acrylic acid) was a sharp drop in modulus from 225 kPa to 45 kPa observed with the lower modulus persisting with further increases in pH. No significant change in modulus was observed across the entire pH range for the unexposed gels, due to the lack of charge in the network. These data indicate that the

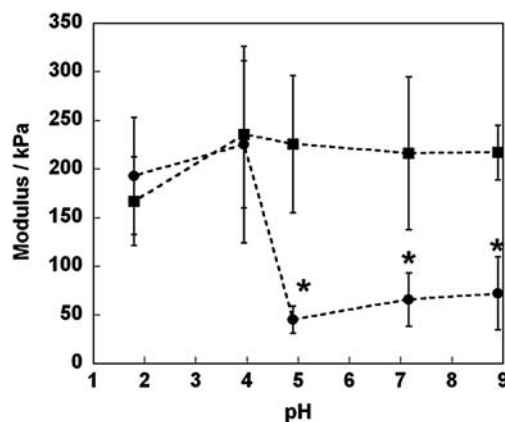


**Fig. 4** Dependence of the elastic modulus for UV-exposed (circles) and unexposed (squares) films on solution pH. \* denotes  $p < 0.0005$  compared to all unexposed samples and the exposed samples at  $\text{pH} < 4.0$ .

predominant factor in driving swelling of the gels, as well as the resulting decreased modulus, is the high charge density generated during the photolysis reaction and subsequent immersion in near-neutral buffer.

### Surface wrinkling

The tethering of the film to the methacrylated glass substrate constrains the in-plane swelling of the film. The resulting anisotropic swelling creates an in-plane compressive stress, producing crazing patterns that emerge when this compressive stress exceeds a critical value.<sup>28</sup> This compressive stress increases with increasing swelling and decreasing modulus. In our system, crazes formed even in the unexposed films; however, the characteristic wavelength ( $\lambda_c$ ) of the features increased significantly with exposure time (Fig. 1b), which is consistent with swelling and modulus results. For unexposed films,  $\lambda_c = 26.2 \mu\text{m}$ , increasing to  $\lambda_c = 38.6 \mu\text{m}$  at 15 minutes and  $\lambda_c = 153.8 \mu\text{m}$  at 90 minutes exposure. The effect of UV exposure on  $\lambda_c$  can be well described by the theoretical model present in the literature,<sup>29</sup> which predicts that  $\lambda_c$  increases linearly with swollen gel height and the inverse fourth root of the elastic modulus. Additional changes to the wrinkling (*i.e.* wavelength, shape) could be induced through alterations of the initial gel thickness and crosslinking density (not shown).

### Cellular response to light-responsive gels

The development of novel substrates for cell culture and growth is of great importance to the field of tissue engineering. To assess

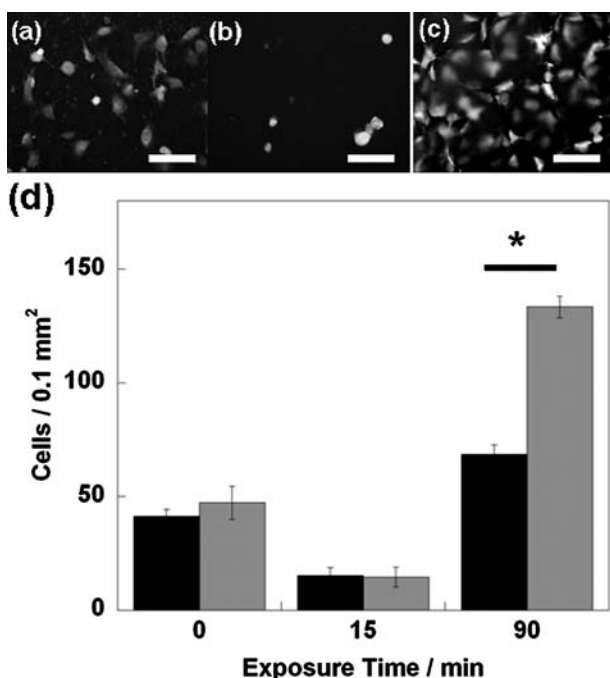


**Fig. 5** Fluorescent images of cells 48 hours after seeding on fibronectin-coated films exposed to UV for (a) 0, (b) 15, or (c) 90 minutes. Scale bars = 50  $\mu\text{m}$ . (d) Average cell density on films 24 (black) or 48 (grey) hours after seeding. Data are presented as  $\pm$ SEM. \* denotes  $p < 0.005$ .  $p < 0.005$  between all exposure times at each time point.

if our photo-responsive gel system might be useful for creating surfaces to modulate cell behavior, we incubated fluorescently stained 3T3 fibroblasts on fibronectin-coated films. Gel incubation with fibronectin prior to cell culture was necessary because of the poor cell attachment we observed for all gel formulations in the absence of the fibronectin (data not shown). This suggests that the 20% addition of 2-NBA did not make the gels sufficiently hydrophobic for serum protein adsorption and cell binding, yet binding may be improved with fibronectin as has been performed previously.<sup>26,30</sup> Images of cells incubated on fibronectin-coated gels were collected at 24 and 48 hours and quantified for cell density (Fig. 5). Because fibronectin adsorption increases with increasing hydrophobicity, we expected to see maximal cell attachment and growth on unexposed gels.<sup>31</sup> Interestingly, we found that gels exposed for 90 minutes best promoted attachment and proliferation with the majority of cells spread. Additionally, the trend of attachment and growth did not follow exposure time. Minimal attachment and growth was observed for 15 minutes exposed gels with nearly all cells being rounded, and unexposed gels showed slightly improved attachment—a combination of rounded and spread cells—but negligible growth was directly observed.

These data taken together suggest a pleiotropic effect of UV irradiation on cell behavior caused by two competing forces for fibronectin interactions. With short irradiation times (*i.e.*, 15 minutes), the gels assume a more hydrophilic surface character (such as indicated by contact angle measurements), thereby resisting protein adsorption. This increased hydrophilicity explains the drop in cell attachment following 15 minutes of exposure. However, with longer irradiation times (*i.e.*, 90 minutes), although gels exhibit increased surface hydrophilicity, the ability of these gels to swell promotes further uptake of the fibronectin and retention, potentially allowing for greater cell binding and proliferation (prior studies demonstrate uptake of fibronectin through chemically similar HEMA gels<sup>26</sup>). The lack of an increase in cell number observed for cells on unexposed films is possibly explained by the combination of some cells proliferating and others becoming detached from the gels with fibronectin desorption. We believe this to be the first demonstration of simultaneous control of surface adhesivity and mechanical stiffness. Light exposure clearly influences cellular interactions on these gels, but the response needs to be optimized for the specific cell types and applications.

### Applications

Materials with spatially and temporally tunable properties are of great interest for applications in tissue engineering. Substrate mechanics, topography and chemistry are all known to influence cellular behavior.<sup>10,26,32</sup> We present here, a system in which all three can be controlled simultaneously. While prior work with light-induced changes in substrate mechanics has involved the breaking of crosslinks, ultimately leading to material failure and often just an erosion of the hydrogel due to limited light penetration,<sup>14,20</sup> our system involves the generation of a high charge concentration, driving the introduction of water and reduction in mechanical stiffness. Additionally, while not demonstrated here, the generation of carboxylic acids could allow for further functionalization of the gel with biologically relevant molecules such

as peptides through amidation chemistry, enabling coupling of mechanics and surface-ligand presentation.<sup>23</sup> Shorter exposure times that do not significantly affect mechanics could be used to generate surface carboxyls for ligand presentation without changing the underlying mechanics, similar to what has been previously demonstrated.<sup>33</sup>

A major advantage of systems that are modulated by controlled light exposure is the ability to define spatial patterns through the use of photomasks.<sup>15</sup> Fig. 6 demonstrates the ability to pattern hydrophilicity and swelling in our gel system using a TEM grid as a photomask. We observed the formation of high-fidelity patterns with depressed regions along the lines of the grid and large swollen regions in the exposed areas. Since  $\lambda_c$  for these gels is longer than the patterned square size, these regions have generally flat surfaces free of the wrinkling characteristic observed for fully exposed gels. However, the exposed regions did exhibit stresses perpendicular to the surrounding unexposed regions, presumably caused by the sudden change in local swelling. The ability to spatially pattern these gels with high fidelity indicates that these materials could be useful for directing cell behavior through generation of regions of variable adhesion, mechanics, topography, or other biological functionality, or for directing further self-assembly of biological materials, as has been demonstrated with PDMS and patterned glass substrates.<sup>34,35</sup>

Recent work from our lab has characterized the dependence of mesenchymal stem cell differentiation on surface topography.<sup>26</sup> Cells that aligned with swelling-induced wrinkles preferentially differentiated down an osteogenic lineage, while those that remained rounded adopted an adipogenic phenotype. Selective, patterned exposure of our gels could induce similar effects, spatially confining cells through swelling-induced topography to certain regions of higher (or lower) modulus, to further control differentiation. Additionally, casting of the gels on deformable substrates could allow further manipulation of the topography through uni-dimensional stretching of the substrate and corresponding alignment of the wrinkles.

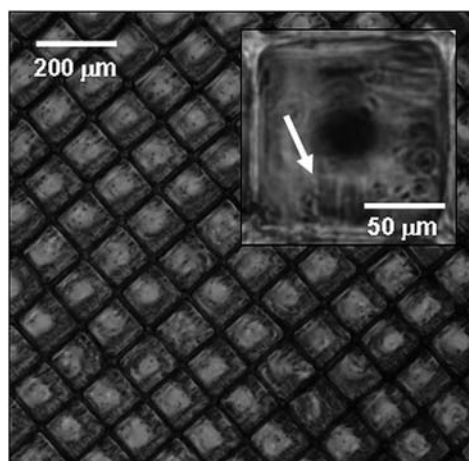


**Fig. 6** Pattern formation caused by differential swelling of the hydrogel following selective irradiation of the gel surface using a TEM grid as a photomask. Swelling-induced strain is visible within individual squares (inset, arrow).

## Conclusion

We have presented the characterization of a novel gel system consisting of the copolymer poly(HEA-co-2-NBA). This system provides a route to the development of gels that can be modulated in hydrophilicity, surface topography, and mechanical stiffness through the use of intermittent UV light exposure. Adhesion and proliferation of 3T3 cells cultured on these gels were highly sensitive to the surface and bulk properties of the underlying gel, and the use of photomasks allowed for the fabrication of patterns with high fidelity and resolution. Consequently, these materials may be of use for further studies in exploring cell–substrate interactions or for controlling cell fates *in vitro*.

## Acknowledgements

This work was funded by the National Science Foundation through a MRSEC at the University of Pennsylvania, a CAREER award (J.A.B.), an REU program (E.R.C.) and a Graduate Research Fellowship (J.S.K.), as well as through a Fellowship in Science and Engineering from the David and Lucile Packard Foundation. The authors acknowledge Dr Harini Sundararaghavan for assistance with the cell staining protocol.

## References

- 1 K. Jain, M. Zemel and M. Klosner, *Proc. IEEE*, 2002, **90**, 1681–1688.
- 2 F. Romanato, L. Businaro, L. Vaccari, S. Cabrini, P. Candeloro, M. De Vittorio, A. Passaseo, M. T. Todaro, R. Cingolani, E. Cattaruzza, M. Galli, C. Andreani and E. Di Fabrizio, *Microelectron. Eng.*, 2003, **67–68**, 479–486.
- 3 H. J. Hou, W. Kim, M. Grunlan and A. Han, *J. Micromech. Microeng.*, 2009, **19**, 127001.
- 4 S. Sarkar, M. Dadhania, P. Rourke, T. A. Desai and J. Y. Wong, *Acta Biomater.*, 2005, **1**, 93–100.
- 5 W. S. Koegler and L. G. Griffith, *Biomaterials*, 2004, **25**, 2819–2830.
- 6 P. Krsko, T. E. McCann, T. T. Thach, T. L. Laabs, H. M. Geller and M. R. Libera, *Biomaterials*, 2009, **30**, 721–729.
- 7 R. A. Marklein and J. A. Burdick, *Adv. Mater.*, 2010, **22**, 175–189.
- 8 R. A. Marklein and J. A. Burdick, *Soft Matter*, 2010, **6**, 136–143.
- 9 Y. Luo and M. S. Shoichet, *Nat. Mater.*, 2004, **3**, 249–253.
- 10 Y. M. Liu, S. Sun, S. Singha, M. R. Cho and R. J. Gordon, *Biomaterials*, 2005, **26**, 4597–4605.
- 11 S. J. Bryant, J. L. Cuy, K. D. Hauch and B. D. Ratner, *Biomaterials*, 2007, **28**, 2978–2986.
- 12 J. Doh and D. J. Irvine, *Proc. Natl. Acad. Sci. U. S. A.*, 2006, **103**, 5700–5705.
- 13 D. S. Shin, K. N. Lee, K. H. Janga, J. K. Kim, W. J. Chung, Y. K. Kim and Y. S. Lee, *Biosens. Bioelectron.*, 2003, **19**, 485–494.
- 14 A. M. Kloxin, A. M. Kasko, C. N. Salinas and K. S. Anseth, *Science*, 2009, **324**, 59–63.
- 15 J. S. Katz and J. A. Burdick, *Macromol. Biosci.*, 2010, **10**, 339–348.
- 16 J. Edahiro, K. Sumaru, Y. Tada, K. Ohi, T. Takagi, M. Kameda, T. Shinbo, T. Kanamori and Y. Yoshimi, *Biomacromolecules*, 2005, **6**, 970–974.
- 17 A. M. Kloxin, J. A. Benton and K. S. Anseth, *Biomaterials*, 2010, **31**, 1–8.
- 18 A. A. Brown, O. Azzaroni and W. T. S. Huck, *Langmuir*, 2009, **25**, 1744–1749.
- 19 J. A. Johnson, M. G. Finn, J. T. Koberstein and N. J. Turro, *Macromolecules*, 2007, **40**, 3589–3598.
- 20 A. M. Kloxin, M. W. Tibbitt, A. M. Kasko, J. A. Fairbairn and K. S. Anseth, *Adv. Mater.*, 2010, **22**, 61–66.
- 21 L. Ionov and S. Diez, *J. Am. Chem. Soc.*, 2009, **131**, 13315–13319.
- 22 S. M. Jay and W. M. Saltzman, *Nat. Biotechnol.*, 2009, **27**, 543–544.
- 23 J. S. Katz, J. Doh and D. J. Irvine, *Langmuir*, 2006, **22**, 353–359.

- 
- 24 Y. Kikuchi, J. Nakanishi, H. Nakayama, T. Shimizu, Y. Yoshino, K. Yamaguchi, Y. Yoshida and Y. Horiike, *Chem. Lett.*, 2008, **37**, 1062–1063.
- 25 D. Blanc, S. Pelissier and P. Y. Jurine, *J. Sol-Gel Sci. Technol.*, 2003, **27**, 215–220.
- 26 M. Guvendiren and J. A. Burdick, *Biomaterials*, 2010, **31**, 6511–6518.
- 27 H. Kaczmarek, A. Szalla, H. Chaberska and J. Kowalonek, *Surf. Sci.*, 2004, **566**, 560–565.
- 28 M. Guvendiren, S. Yang and J. A. Burdick, *Adv. Funct. Mater.*, 2009, **19**, 3038–3045.
- 29 H. Tanaka, H. Tomita, A. Takasu, T. Hayashi and T. Nishi, *Phys. Rev. Lett.*, 1992, **68**, 2794–2797.
- 30 C. R. Nuttelman, D. J. Mortisen, S. M. Henry and K. S. Anseth, *J. Biomed. Mater. Res.*, 2001, **57**, 217–223.
- 31 T. A. Horbett, in *Biomaterials Science*, ed. B. D. Ratner, A. S. Hoffman, F. J. Schoen and J. E. Lemons, Elsevier Academic Press, 2004.
- 32 A. J. Engler, S. Sen, H. L. Sweeney and D. E. Discher, *Cell*, 2006, **126**, 677–689.
- 33 M. S. Hahn, J. S. Miller and J. L. West, *Adv. Mater.*, 2006, **18**, 2679–2684.
- 34 Y. Du, M. Ghodousi, E. Lo, M. K. Vidula, O. Emiroglu and A. Khademhosseini, *Biotechnol. Bioeng.*, 2008, **105**, 655–662.
- 35 J. G. Fernandez and A. Khademhosseini, *Adv. Mater.*, 2010, **22**, 2538–2541.